

Sulfidation, down-time corrosion and corrosion-assisted cracking on high alloy materials in synthetic coal gasifier environments

W. M. M. Huijbregts* , E. Kokmeijer* and H. G. van Zuilen*

Materials for Coal Gasification Power Plant, International Workshop Petten, 14-16 June 1993. (paper 41)

* KEMA Inspection Technology, Utrechtseweg 310, 6812 AR Arnhem, The Netherlands

Summary.

At the KEMA laboratories, three types of corrosion concerning heat exchangers in coal gasifiers were studied in detail:

- resistance of materials to general corrosion (sulfidation);
- down-time corrosion;
- interaction between stress/strain and corrosion (corrosion-assisted cracking).

A combination of optical and scanning electron microscopy and special sample preparation techniques gave excellent information about the corrosion mechanisms of sulfidation and down-time corrosion. The slow strain rate testing technique was applied to classify materials according to resistance to corrosion-assisted cracking. Critical temperatures for cracking were determined.

Introduction

Coal gasification in combination with steam and gas turbines is a very attractive technique for the production of electrical energy. An important factor in making coal gasification a success is the choice of reliable materials. There are three main areas of concern for materials used in heat exchangers: resistance of materials to general corrosion (sulfidation); down-time corrosion (DTC); and interaction between stress/strain and corrosion (corrosion-assisted cracking). These three types of corrosion have been studied in detail at the KEMA laboratories. The following materials were the focus of attention: AISI 310, Alloy 800, Sanicro 28, AC 66 and Cr diffusion coatings on 10CrMo9.10.

Experimental and the results

The steels and the gasifier environments discussed in this paper are summarized in Tables 1 and 2.

Table 1 Compositions of materials (wt%)

Material	Cr	Ni	Mo	Cu	C	Si	Mn	Other
10CrMo9.10	2.3		1.0	0.1	0.15	0.3	0.4	
Mod9Cr1Mo	8.8		1.0		0.12	0.4	0.4	
AISI 347	18	11			0.08	0.5	1	
AISI 446	25				0.20	0.5	0.8	
AISI 310	25	20			0.25	0.8	1	
AISI 310Nb	25	20			0.08	0.8	1	1% Nb
Alloy 800	21	32		<0.8	<0.1	0.5		0.4% Ti + 0.4% Al
Alloy 800H	21	32			<0.10	0.8		0.4% Ti + 0.4% Al
Sanicro 28	27	31		1	<0.02			
AC 66	27	32			0.06	0.2	0.5	0.07% Ce + 0.8% Nb

Table 2 Composition of gasifier environments studied (volume fraction)

Gas	CO	CO2	H2	H2S	H2O	HCl	Ar	N2	Pressure (MPa)	Comments
Ref 1	0.621	0.02	0.281	0.010	0.002				0.1	See Fig 7
Ref 2	0.444	0.099	0.296	0.006					0.1	See Fig 7
Lab no.5			.0190	0.010	0.015		0.785		0.1	SSR test
Lab no. 7	0.277	0.058	0.164	0.001	0.008		0.500		0.1	SSR test
CRE PP11	0.160	0.100	0.120	0.0013	0.100			0.60	0.1	Plant exposure
REE PG0	0.090	0.130	0.140	0.003		0.005		0.63	1.2	Plant exposure

The gases Ref 1 and Ref 2 are mentioned because they were used as reference gases to calculate corrosion rates in the other gases, gases no.5 and no.7, that were applied in the laboratory experiments. CRE PPII and CRE PGO are gas compositions from the plant exposures in the Coal Research Establishment (CRE) of the British Coal Corporation.

Sulfidation in plant exposure

A number of stainless steels were exposed in the laboratory and in the atmospheric and the high pressure gasifier at the CRE. Uncooled samples were exposed during run PPII (atmospheric gasifier) and during run PGO (1.2 MPa gasifier). No special precautions against DTC were taken during shutdown periods. The materials were exposed at 480 °C for 834 h in run PPII and for only 192 h in run PGO. Some interesting corrosion aspects of Sanicro 28 and AISI 310 will be discussed.

In Figure 1 the maximum thickness of the corrosion scale and maximum depths of pitting and intergranular attack (IGA) are shown. These corrosion data are derived from microscopic examination of cross-sections of the samples.

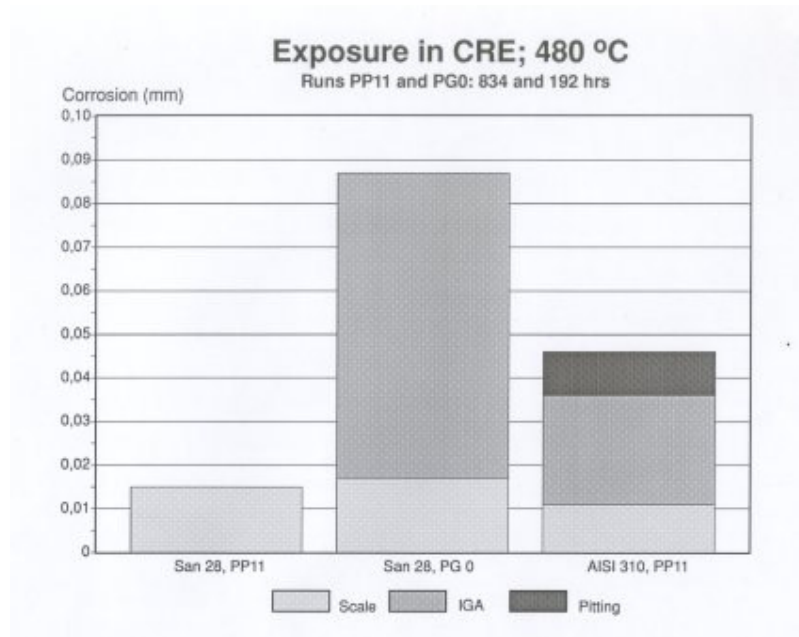


Figure 1 Corrosion on Sanicro 28 and AISI 310 exposed at 480 °C (runs PP11 and PG0)

In addition to scanning electron microscopy (SEM) equipped with wave dispersive scanning (WDS) and energy dispersive scanning (EDS), the specimens were also studied by means of double interference contrast optical microscopy (DICOM). In the latter technique the samples are coated with a 6 micron ZnS layer and examined by using interference contrast optical microscopy. The various phases in the corrosion scale can be distinguished by means of the differences in colour. The SEM photographs are shown in Figures 2 and 3 in black and white.

Sanicro 28.

The corrosion scale consists of three layers (see Figure 2a): an outer layer consisting mainly of FeS (1), a topotactical 'porous' oxide layer (3) and in between a Cr-rich sulfide layer (2). Porosity in the topotactical layer starts about 0.5 micron behind the oxide- metal interface. From research with the SEM/WDS and the DICOM technique it appears that this porosity may be filled with sulfides. The porous layer is considered to be mixed with sulfides. Internal sulfidation was found at some locations.

The Sanicro 28 was corroded intergranularly as a result of DTC in the sample that was exposed in run PGO, in which the chloride content was higher (see Figure 2b).

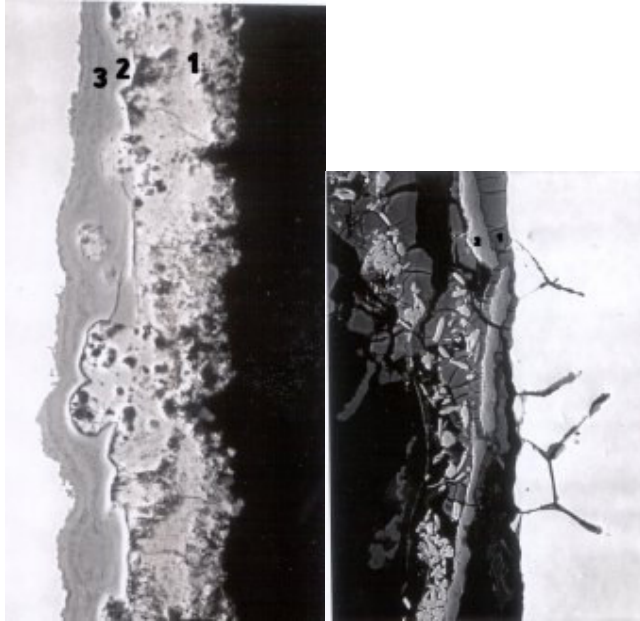


Figure 2. SEM photographs of Sanicro 28 at locations also examined by DICOM. (upper figure) Adherent corrosion scale consisting of three layers. (lower figure) Scale detached and down-time corrosion with intergranular attack.

At locations where this type of corrosion occurred a clay-like structure (1) was found between the topotactical corrosion scale (2) and the steel. Intergranular corrosion occurred under the 'clay'. This 'clay' had a high Mo, O and Cl content. It is well known from stainless steels that in the case of pitting corrosion of Mo-containing steels, a very acid MoCl complex is formed in the pits; the intergranular corrosion rate is very fast in such a situation.

AISI 310.

The corrosion scale of AISI 310 has a topotactical and an epitactical layer. The topotactical layer is porous and at some locations it has blisters. The pores and blisters are filled with FeS. The epitactical layer consists mainly of coarse crystalline FeS (see Figures 3a and 3b). The difference between AISI 310 and the Sanicro 28 material is the lack of the Cr-rich sulfide layer between the topotactical and the epitactical layer. Pitting corrosion and some IGA was found. By means of the DICOM technique, sulfide penetration was detected at the grain boundaries. AISI 310 was not exposed at 480 °C in run PGO. DTC was not found on this specimen.

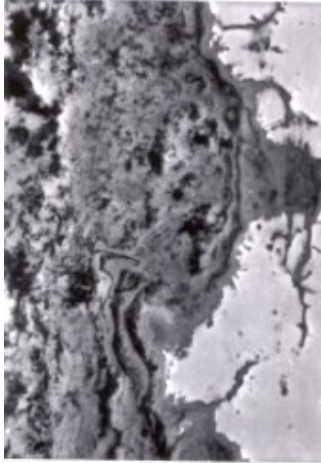


Figure 3. SEM photographs of AISI 310 at locations also examined by DICOM. (a) The topotactical porous layer and the epitaxial FeS layer. (b) In the porous layer blisters are also found. Sulfides are present at the grain boundaries

Down-time corrosion

To simulate DTC the EPRI corrosion test is applied [1]. In this test, fly ash from a coal gasifier was deposited on the specimens together with the eutectic salt mixture, 37.4% NaCl and 62.6% FeCl₂. The specimens (various melts of the materials) were exposed to humid air at a temperature of 70 °C for 24 h. The specimens were examined by optical microscopy and the deepest pits were measured. The results of the DTC experiments are summarized in Figure 4.

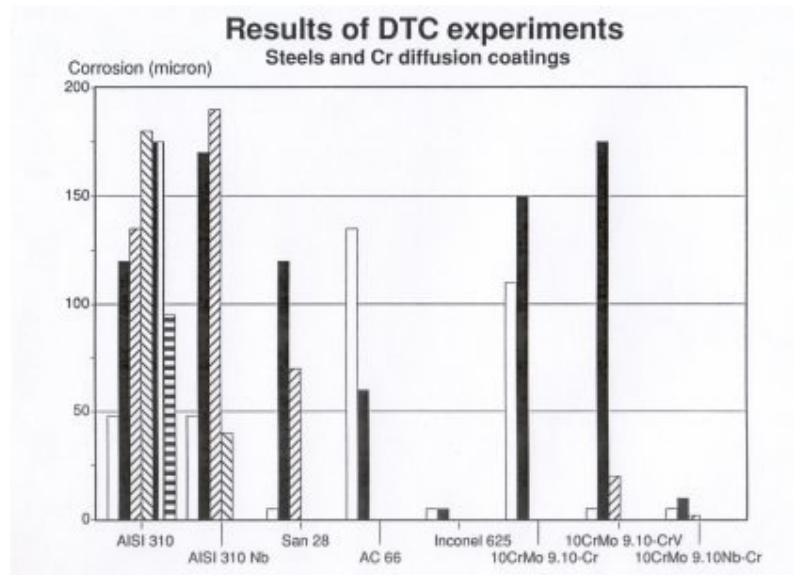


Figure 4 Results of DTC experiments on steels and Cr diffusion coatings

Slow strain rate tensile test in corrosive environments

In slow strain rate (SSR) experiments tensile specimens are strained at a constant, slow rate in two corrosive atmospheres: gases no.5 and no.7 in Table 2. The temperature ranged from 400 to 550 °C.

The extension rate was 16×10^{-7} /s for most of the experiments. Depending on the fracture strain of the steel, a test took about 3 days. The gas flow was 21 h⁻¹. Three atmospheric and one high pressure SSR machine were available for the tests. A total of 200 experiments were performed on various materials. It is not possible to present here all the results on fracture strains, etc.

During the course of the project a correlation between cracking, strain, tensile stress and area reduction was sought. None was found. However, detailed microscopic examination of the specimens showed that in corrosive gases cracks were formed along the length of the tensile specimen. Some examples of the different cracking phenomena are given in Figures 5 and 6. It appears that the cracking pattern changed with test temperature. Based on cracking appearance the specimens were classified as follows.

- Class 1: no cracks found. Sometimes superficial notches were formed along the length of the specimen, particularly in the case of steels with high strain, such as the austenitic materials. These notches were not considered to be real cracks (Figures 5a and 6a).
- Class 2: cracks detected in the area of reduction only (Figure 5b).
- Class 3: cracks present over the entire length of the specimen (Figures 5c, 6b and 6c).

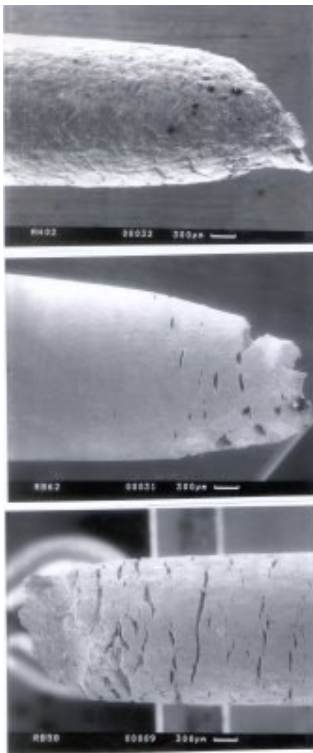


Figure 5

Examples of the three classes of cracking.

Class 1 - notches only: Sanicro 28 at 450 °C.

Class 2 cracks in the area of reduction' 10CrMo9.10 at 450 °C.

Class 3 -cracks along the length of the specimen: Alloy 800 at 475 °C

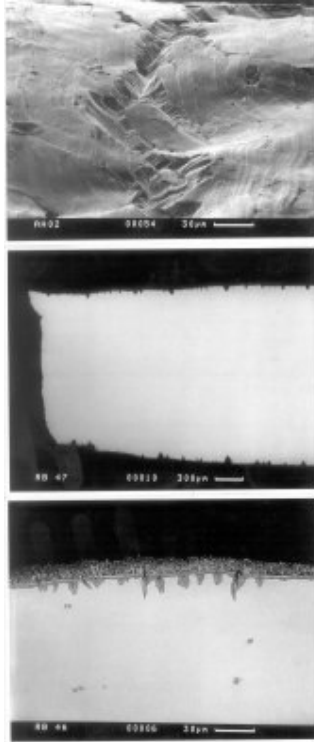


Figure 6 Details of slow strain rate samples.

- a. SEM photomicro- graph. notch in Sanicro 28.
- b. Cross-section of Alloy 800: class 3 crack.
- c. Detail of cracks in Alloy 800

Discussion

Corrosivity of sulfidizing gas

The corrosivity of sulfidizing gases is often described in terms of the sulfur and oxygen pressures, calculated from the gas composition by minimizing the thermodynamic potential. However, total equilibrium of the gas can only be achieved at relatively high temperatures [2-4]. At lower temperatures ($< 1100\text{ }^{\circ}\text{C}$) the gas composition is 'frozen' and the non-equilibrium partial pressures of oxygen and sulfur can be calculated from the CO/CO_2 equilibrium constant and $\text{H}_2/\text{H}_2\text{S}$ equilibrium constant, respectively. According to John [3,4] the corrosion of Alloy 800 in sulfidizing gas is parabolic and the corrosion factor k is dependent not only on the activation energy but also on the sulfur and oxygen partial pressures.

$$X^2 = kt$$

$$\log k = \log k_0 + 0.09(\log p_{\text{S}_2} - 1.51 \log p_{\text{O}_2}) - Q/RT$$

$$\log k_0 = 2.78$$

$$Q/R = 5703$$

To obtain an impression of the corrosivity of our various test gas compositions, the corrosion in these gases after 2000 h was calculated by means of the above formulae (see Figure 7). The gases can be ranged in decreasing corrosivity, as follows:

Ref 1, gas no.5, Ref 2, gas no.7, CRE PPII, CRE PGO.

The laboratory gases no.5 and no.7 are applied in our SSR tests. A wider variety of corrosive gases will be chosen at a later stage of research.

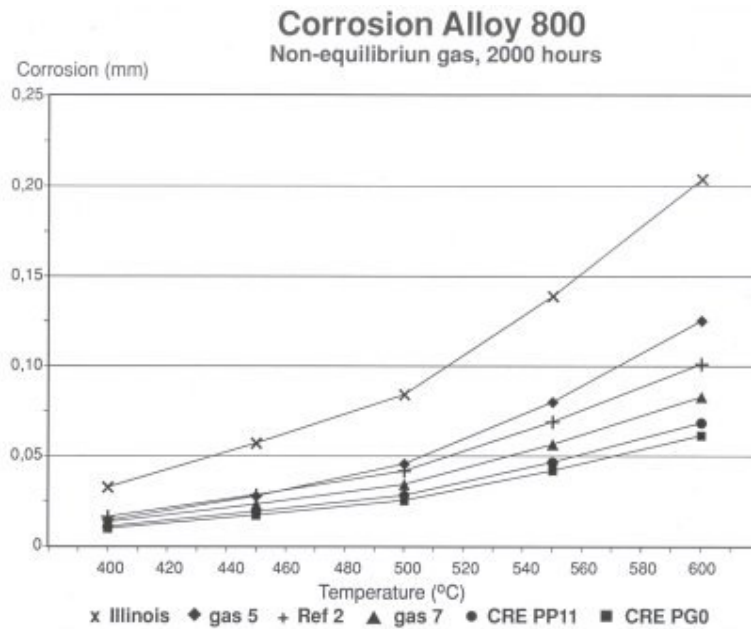
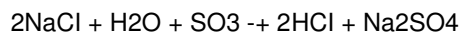


Figure 7. Corrosion of Alloy 800 calculated for non-equilibrium gases after 2000 h.

Down-time corrosion

In the case of DTC three factors are important: chloride, unburned coal and poly thionic acid.

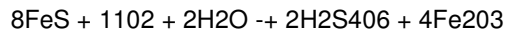
In an oxidizing atmosphere the NaCl present in the coal will react and form sodium sulfate:



The hydrochloric acid will be transported in the flue gas and corrosivity for the evaporator tubes will be minimal. In coal gasifiers the transition into HCl will not be complete and the NaCl can be deposited, together with some unburned coal, on the heat exchangers. At relatively low HCl concentrations, FeCl₂ is stable and can be formed on the metal-oxide interface. It is even possible that low-melting eutectic salts are formed. The NaCl-FeCl₂ eutectic has a melting point of 270 °C.

The unburned coal on the metal surfaces is very cathodic, and during shutdown periods or in combination with the eutectic salts depolarizing of the cathodic reaction will result in high corrosion rates. Pitting corrosion can be severe.

During shutdown periods the FeS in deposits can be oxidized to form poly thionic acid:



Polythionic acid is a very aggressive acid, particularly for sensitized steels. Intergranular corrosion by poly thionic acid is a well-known cause of damage. The effect of poly thionic acid was not included in the EPRI test; nevertheless, the test is rather aggressive because of the chloride present (Ref 1).

Various classes were introduced to describe resistance to DTC; they are listed in Table 3.

No precautions were taken for DTC in the CRE gasifier. It appeared that the steels that had DTC damage after exposure in the CRE gasifier were corroded in the EPRI test to a depth of more than 50 μm (classes 4 and 5). From Figure 4 it would appear that there is a rather wide variation in corrosion for the Sanicro 28 and the CrV diffusion coatings on 10CrMo9.10. Materials in classes 1-3 (Table 3; Inconel 625 and Cr diffusion coating on Nb-stabilized IOCrMo9.10) will provide a much lower risk of DTC.

Table 3 Classifications describing resistance to down-time corrosion

Class	Attack in steel	Attack in coatings
1	No attack	No attack
2	0-10 micron	Attack of carbide layer
3	10-50 micron	< 20% of coating
4	50-100 micron	> 20% of coating
5	100-200 micron	
6	> 200 micron	

Slow strain rate

The SSR test is considered somewhat appropriate for fast testing and ranking of materials on resistance to corrosion-assisted cracking. We were interested in determining the critical temperatures at which the materials had cracking patterns of classes 1, 2 and 3. These critical temperatures are summarized in Table 4.

Ferritic materials

In some supercritical boilers in the USA cracking was detected in the waterwalls. These boilers operate at metal temperatures higher than normally applied in subcritical boilers. The circumferential cracks in the IOCrMo9.10 tubes were filled with magnetite and sulfides, indicating the presence of a sulfidizing atmosphere. There are several names for this type of cracking: alligator skin cracking (ASC), alligating, grooving, waterwall cracking and elephant hiding [5]. The critical temperatures for cracking of classes 1, 2 and 3 are named ASC-1, ASC-2 and ASC-3, respectively.

The mechanism of ASC is summarized by Smith and Marder [5]:

- initiation of intergranular corrosion and sulfidation on the grain boundaries
- because of high heat fluxes, compressive stresses on the outer tube metal surface and plastic deformation take place at high stresses
- at lower heat fluxes, residual stresses are present
- because of intergranular penetration there is stress concentration on the crack tip during thermal cycling
- propagation of the crack and sulfidation on the crack tip

The cracks found in our SSR experiments in 10CrMo9.10 (Figure 5b) are rather similar to those found in some waterwall tubes. The possibility of ASC is a reason for concern if 10CrMo9.10 steel is

applied for evaporators in sulfidizing atmospheres that may occur when low NO_x firing techniques are used. A CrY diffusion coating is more resistant to ASC as well as to DTC [5].

The Mod9Cr1Mo material also has a rather low ASC-3 temperature (400°C), but the ASC-1 and ASC-2 temperatures of AISI 446 are rather high: 450 and 500°C, respectively.

Austenitic materials

The materials AISI 310, Alloy 800H and Alloy 800 have ASC-3 temperatures lower than 450°C; AISI 310 has a value even lower than 400°C. AISI 347 probably has a better resistance, because the ASC-2 temperature is 450°C. The ASC-1 temperatures remain to be determined for these materials.

Table 4 Types of cracking in slow strain rate experiments

Material	Class of cracking at temperature (°C)						
	350	400	425	450	475	500	550
10CrMo9.10		2		2			
Mod9Cr1Mo		3		3			
AISI 446				1		2	
AISI 347		1	2	2		3	3
AISI 310	3	3	3	3	3		3
AISI 310Nb							
Alloy 800			3	3	3		
Alloy 800H		3	3	3			
Sanicro 28			1	1	3	3	3
AC 66				1	3	3	3

Hill and Black [6] and Wells et al. [7] did creep experiments in gasifier atmospheres at 6.8 MPa and at 650°C and above on the materials Alloy 800H and AISI 310. The fracture times became shorter in gasifier conditions and the toughness was largely reduced. The mechanism is internal sulfidation under a thin layer of Cr₂O₃ and transformation of Cr carbides to sulfides.

The toughness and fracture behaviour of the 'protective' corrosion scale are important factors. If the layer is fractured, Cr-depleted zones and grain boundaries will be particularly sensitive to fast attack. At these temperatures and sulfidizing atmospheres it should not be ruled out that the topotactical layer grows under compressive stress. Formation of pores in, and blistering of, the oxide layer is possible and will reduce the protection provided by the oxide layer [7].

The exposure tests in CRE showed that intergranular sulfidation occurred underneath the porous and blistered topotactical corrosion scale of AISI 310, even under stress-free conditions (see Figure 3). It is quite probable that the slightest intergranular and internal sulfidation under slow strain rate conditions will initiate intergranular cracking. The ASC-1 and/or the ASC-2 temperature probably coincides with the temperature at which internal sulfidation does not yet occur.

The materials Sanicro 28 and AC 66 are better materials regarding corrosion-assisted cracking. The ASC-3 temperature for Sanicro 28 and AC 66 is 475°C. More experiments are needed to determine the exact ASC-2 value. The better resistance of these materials can be explained by the good quality of their oxide layer. Internal sulfidation does not occur at these low temperatures.

Conclusions

- Corrosivity of sulfidizing gases may be compared by calculating the corrosion of Alloy 800 applying non-equilibrium partial pressures for oxygen and sulfur. However, published corrosion data to support calculated corrosion rates are scarce.
- Down-time corrosion can be disastrous for some materials, because it may initiate pitting as well as intergranular corrosion. The EPRI test is an inexpensive technique for ranking materials on DTC resistance. The test, however, may be too severe if down-time corrosion is limited by appropriate operating techniques.
- Materials exposed in pilot plants provide good information about the DTC mechanism as well as information about general corrosion. A combination of DICOM and SEM equipped with EDS and WDS gives excellent information.
- The SSR experiment in sulfidizing atmospheres is appropriate for fast testing of materials for their resistance to corrosion-assisted cracking. Internal sulfidation on the grain boundaries may initiate the cracking.
- The determination of critical ASC temperatures is a promising technique for screening of materials and welds.
- Compared with other materials tested, Sanicro 28 and AC 66 have rather high resistances to corrosion-assisted cracking. The ASC-I temperature ranges between 450 and 475 °C.

Acknowledgement

Plant exposures at the Coal Research Establishment were possible as a result of cooperation in the COST 50 I round 2 WP4 project.

References

1. Perkins, R. A., Marsch, D. L., Sarosiek, A. M. and Bakker, W. T. 'Downtime Corrosion in Syngas Coolers of Entrained Slagging Gasifiers', report AP-5966, Project 2048-1, Topical Report, EPRI, 1988
2. Bakker, W. T. and Perkins, R. A. in 'Chlorine in Coal' (Eds J. Stringer and D. D. Banerjee), Elsevier, Amsterdam, 1991, pp. 63- 80
3. John, R. C. Proceedings of the NACE Conference on Life Prediction of Corrodible Structures, Cambridge, UK, 23-26 September 1991
4. John, R. C. Corrosion 88, St Louis, Missouri, 21-25 March 1988, paper no.136
5. Smith, B. J. and Marder, A. R. J. Eng. Mater. Technol. 1992, 114, 265
6. Hill, V. L. and Black, H. L. 'The Properties and Performance of Materials in the Coal Gasification Environment', Proceedings of a Conference, Pittsburgh, PA, 8-10 September 1980, ASM, 1981
7. Wells, C. H., Zeis, L. A. and Page, R. A. 'The Properties and Performance of Materials in the Coal Gasification Environment', Proceedings of a Conference, Pittsburgh, PA, 8-10 September 1980, ASM, 1981, pp. 5